Propagating transitions of electroconvection

著者	鈴木 誠
journal or publication title	Physical review. A
volume	31
number	4
page range	2548-2555
year	1985
URL	http://hdl.handle.net/10097/35399

doi: 10.1103/PhysRevA.31.2548

PHYSICAL REVIEW A VOLUME 31, NUMBER 4 APRIL 1985

Propagating transitions of electroconvection

Makoto Suzuki
Mechanical Engineering Laboratory, 1-2 Namiki, Sakura-mura, Ibaraki 305, Japan
(Received 15 October 1984)

In a thin dielectric liquid layer, electroconvection can be generated by means of charge injection to the liquid under a vertical electric field. When a parameter which gives the critical condition of the onset of convection is rapidly increased up to some value across the critical point, a propagating transition of the system from the quiescent state to the convecting state is expected to appear. We have tried to show such propagating transitions in two different models. One for a bipolar-injection type with free-free boundaries was analyzed with use of the amplitude-equation approach of Newell and Whitehead, and the other for a unipolar-injection type with rigid-rigid boundaries was numerically analyzed. Both cases have shown propagating transitions of convecting state with definite velocities.

I. INTRODUCTION

In a thin dielectric liquid layer where space charge is formed, electroconvection may be generated in a supercritical condition. In such a system, nonlinear diffusion of the convecting state might be expected. In other convecting systems the Rayleigh-Bénard convection was analyzed by Newell and Whitehead.[1] Their method is applicable to investigate the structures of convection and its diffusional properties near the critical point. Cross[2] and Greenside and Coughran[3] have shown the convective textures of laterally large Rayleigh-Bénard cells using the amplitude equation approach. In Couette-Taylor flow Ahlers and Cannell[4] have experimentally shown that the propagation velocity of the vortex front could be explained from an amplitude equation. On the other hand, electroconvection has been studied by Atten, Lacroix, and their co-workers.[5–7] The electric current versus voltage relations including hysteresis have been explained by a mean-field approximation of a quasilinear type. The structures of convecting cells were discussed by modal stability analysis.[6]

When a parameter which gives the critical condition is rapidly increased up to some value across the critical point, a convecting state will be generated somewhere and finally occupy the whole space of the liquid layer. If the initial inhomogeneity is very small, the growing feature of the convecting state might take a form of a propagating wave front. This is the main motivation of this study. The author has tried to show such propagating transitions in two systems, by analytical and numerical techniques. One model is a bipolar injection type with free-free boundaries, and the other a unipolar injection type with rigid-rigid boundaries.

II. A BIPOLAR INJECTION TYPE WITH FREE-FREE BOUNDARIES

A. Model specifications

When a dielectric Newtonian liquid layer held between $z=d/2$ and $z=-d/2$ is subjected to a bipolar ion injection at $z=\pm d/2$, the liquid shall show a transition of the state by increasing the parameter giving the critical condition. We chose the following symmetrical model against the $z=0$ plane to see the transitional feature of the charged fluid analytically. The detailed specifications of the model is as follows. The boundary conditions are, at $z=-d/2$,

$$\Phi=V_0/2,\ \ n_+=n_0,\ \ w=0,\ \ D^2w=0\ ,$$

and at $z=-d/2$, (2.1)

$$\Phi=-V_0/2,\ \ n_-=n_0,\ \ w=0,\ \ D^2w=0\ ,$$

where Φ, n_+, and n_- denote the electric potential, the positive ion density, and the negative ion density, respectively, and the flow velocity $\mathbf{u}=(u,v,w)$. D represents $\partial/\partial z$. The mobility and the diffusion coefficient of each ion are μ and K in the amplitude, respectively, because of the symmetrical arrangement. The balance equations for both ion densities become

$$\frac{\partial n_+}{\partial t}+\nabla\cdot[n_+(\mu\mathbf{E}+\mathbf{u})-K\nabla n_+]=-\alpha n_+n_-\ , \tag{2.2}$$

$$\frac{\partial n_-}{\partial t}+\nabla\cdot[n_-(-\mu\mathbf{E}+\mathbf{u})-K\nabla n_-]=-\alpha n_+n_-\ , \tag{2.3}$$

where $\mathbf{E}$ denotes the electric field given by

$$\nabla\cdot\mathbf{E}=q/\epsilon\ \text{ and }\ \mathbf{E}=-\nabla\Phi\ . \tag{2.4}$$

α is the recombination coefficient, and q the space charge density

$$q=(n_+-n_-)e\ . \tag{2.5}$$

The following two conditions definitely characterize the model:

(1) the weak recombination condition (WR)

$$\alpha \ll \frac{\mu E_0}{n_0 d}\ \ (E_0=V_0/d)\ , \tag{2.6}$$

(2) the weak injection condition (WI)

$$E_0 \gg \left[\frac{e\alpha n_0^2 d^2}{\epsilon\mu} \right]^{1/2} . \tag{2.7}$$

The first condition means that the injected ion densities hardly decrease by recombination in the transit time, though the space charge is produced by recombination. The second condition means that the external electric field is so strong that the field induced by the space charge is negligibly small. In this case ionic drift velocities are usually much larger than the diffusional velocities so that the ionic diffusion terms should be neglected.

B. Analysis

1. *Stationary state*

At the limit of $\alpha \to 0$, the stationary state ($\mathbf{u}_s \equiv \mathbf{0}$, subscript s shows the stationary solution) gives $q_s = 0$. In the WR condition we do not take into consideration the terms of $O(\alpha^2)$ but $O(\alpha)$. Moreover the z dependences of n_{+s} and n_{-s} are very small in the WI condition, so they could be approximated by linear functions of z. Therefore the right-hand side (rhs) of Eq. (2.2), which is the same as (2.3), can be replaced by αn_0^2. The stationary solutions become

$$n_{\pm s} = \pm az + b, \quad E_s = \frac{ea}{\epsilon} z^2 + E_0 , \tag{2.8}$$

where

$$a = -\alpha n_0^2 / \mu E_0 ,$$
$$b = n_0 - \alpha n_0^2 d / 2\mu E_0 .$$

Here the WI condition was used. The αn_0^2 replacements are now justified since $b \gg |a|$ by means of the WR condition.

2. *Near the critical point*

Let us consider small variations around the stationary state. They are denoted by variables with primes as follows.

$$\begin{aligned} &\mathbf{E} = \mathbf{E}_s + \mathbf{E}', \quad \mathbf{u} = \mathbf{u}' , \\ &n_+ = n_{+s} + n'_+, \quad n_- = n_{-s} + n'_- , \\ &\rho_+ = \rho_{+s} + \rho'_+, \quad \rho_{+s} = 2b, \quad \rho'_+ = n'_+ + n'_- , \\ &\rho_- = \rho_{-s} + \rho'_-, \quad \rho_{-s} = 2az, \quad \rho'_- = n'_+ - n'_- . \end{aligned} \tag{2.9}$$

The balance equations of ion densities (2.2) and (2.3) then become

$$\frac{\partial \rho'_+}{\partial t} + \nabla \cdot (\rho_{-s}\mu \mathbf{E}' + \rho_{+s}\mathbf{u} + \rho'_-\mu \mathbf{E}_s + \rho'_-\mu \mathbf{E}' + \rho'_+ \mathbf{u}) = -2\alpha n_0 \rho'_+ , \tag{2.10}$$

$$\frac{\partial \rho'_-}{\partial t} + \nabla \cdot (\rho_{+s}\mu \mathbf{E}' + \rho_{-s}\mathbf{u} + \rho'_+\mu \mathbf{E}_s + \rho'_+\mu \mathbf{E}' + \rho'_- \mathbf{u}) = 0 , \tag{2.11}$$

where terms of $O(\alpha^2)$ and second order of variations multiplied by α were all neglected. Moreover we neglect the terms of second order of variations including the electric field due to the space charge caused by the WI condition. Then $\mathbf{u}$ is governed by the Navier-Stokes equation

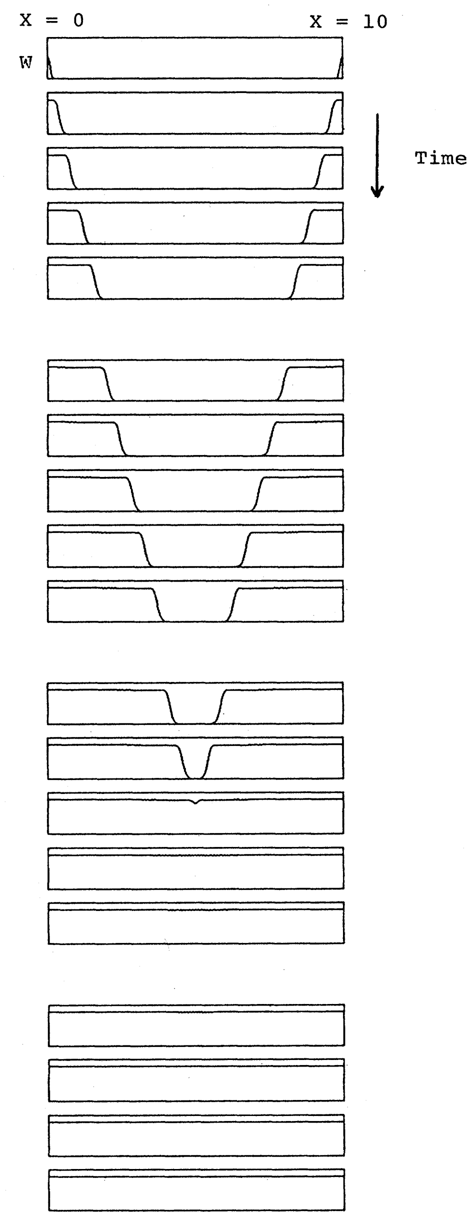

FIG. 1. Nonlinear diffusion obtained from Eq. (2.31). The convecting state was initiated at the side walls and propagated to the inner region. The figures show the time lapse downward with time step $\Delta T = 0.25$.

$$\frac{\partial \mathbf{u}}{\partial t}+(\boldsymbol{\Omega}\times\mathbf{u})=-\nabla\left[\frac{p}{\rho}+\tfrac{1}{2}\mathbf{u}\cdot\mathbf{u}\right]+\frac{1}{\rho}qE_0\hat{z}+\nu\Delta u$$

and

$$\nabla\cdot\mathbf{u}=0 . \tag{2.12}$$

Before rewriting Eqs. (2.10) and (2.11) we assume the form of the neutral solution w_0 or q_0 as

$$(We^{i\mathbf{k}\cdot\mathbf{x}}+W^*e^{-i\mathbf{k}\cdot\mathbf{x}})\sin(\pi z/d) .$$

Then ρ'_{-0} should take the same form. Therefore n_{+0} and n'_{-0} are given by

$$n'_{\pm 0}=\left[n'_0\cos\left[\theta\mp\frac{\pi z}{d}\right]+n'_0\sin\theta\right](We^{i\mathbf{k}\cdot\mathbf{x}}+W^*e^{-i\mathbf{k}\cdot\mathbf{x}}) . \tag{2.13}$$

Then

$$\rho'_{-0}=2n'_0\sin\theta\sin\left[\frac{\pi z}{d}\right](We^{i\mathbf{k}\cdot\mathbf{x}}+W^*e^{-i\mathbf{k}\cdot\mathbf{x}}) ,$$

$$D\rho'_{+0}=-\frac{2\pi n'_0}{d}\cos\theta\sin\left[\frac{\pi z}{d}\right](We^{i\mathbf{k}\cdot\mathbf{x}}+W^*e^{-i\mathbf{k}\cdot\mathbf{x}}) . \tag{2.14}$$

Therefore Eq. (2.11) can be rewritten in the WR and WI conditions near the critical point as

$$\frac{\partial q}{\partial t}+\mathbf{u}\cdot\nabla q-\beta w=-\gamma q , \tag{2.15}$$

where

$$\gamma=\frac{\pi^2\mu^2E_0^2}{2\alpha n_0 d^2} ,$$
$$\beta=\frac{2\alpha n_0^2 e}{\mu E_0} , \tag{2.16}$$

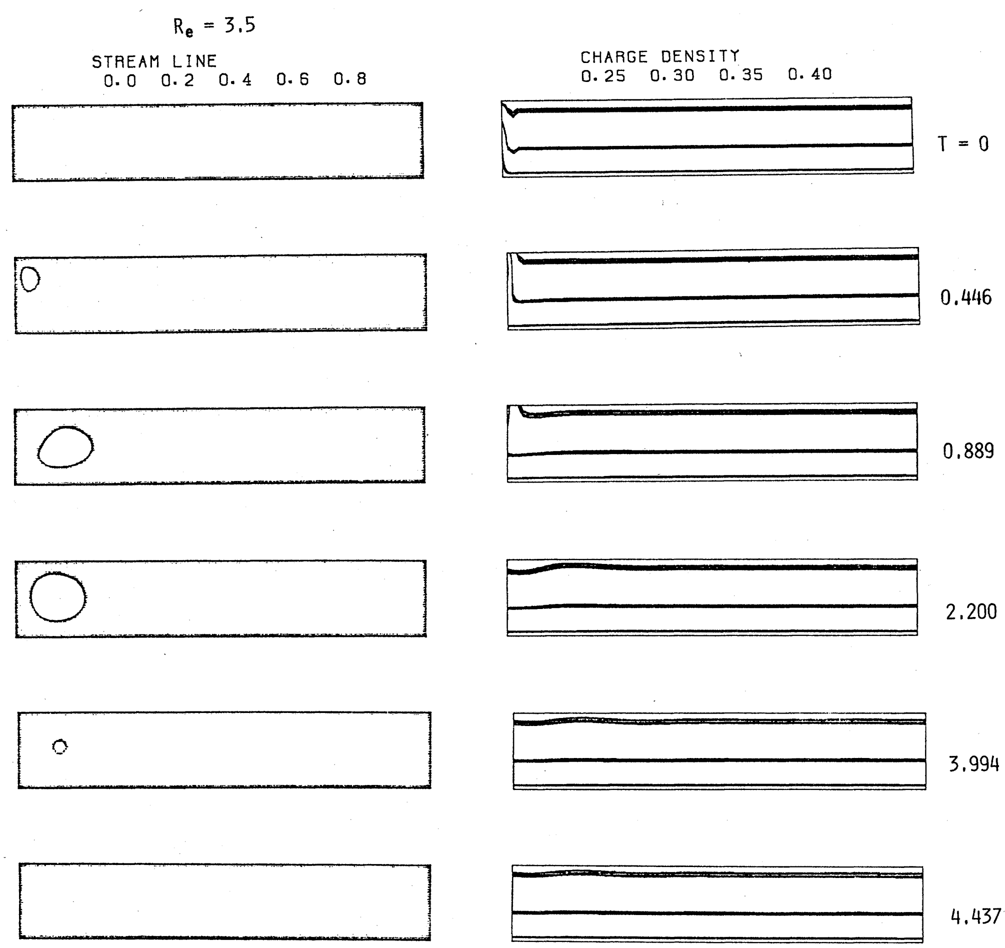

FIG. 2. Relaxation of convecting state below the critical point, electric Reynolds number $R_e=3.5<3.926$. Positive charges were injected at the bottom. After the space charge was modulated at the left side, the convection was generated temporarily and relaxed afterward.

and

$$\cot\theta = -\frac{\pi\mu E_0}{2\alpha n_0 d} ,$$

which was found from Eq. (2.10) after linearization at the steady condition. The equation set (2.12) and (2.15) is reduced to a single equation by twice taking the curl and taking its dot product with $\hat{z}$, the unit vector in the z direction, and applying the operator $(\partial/\partial t+\gamma)$

$$\left[\frac{\partial}{\partial t}-\nu\Delta\right]\left[\frac{\partial}{\partial t}+\gamma\right]\Delta w-\frac{g}{\rho}\nabla_1^2 w=-\frac{E_0}{\rho}\nabla_1^2(\mathbf{u}\cdot\nabla q)+\left[\frac{\partial}{\partial t}+\gamma\right][\hat{z}\cdot(\nabla\times\nabla\times(\boldsymbol{\Omega}\times\mathbf{u}))] , \tag{2.17}$$

where $g=E_0\beta$. According to Newell and Whitehead, we begin with the following modified neutral solutions:

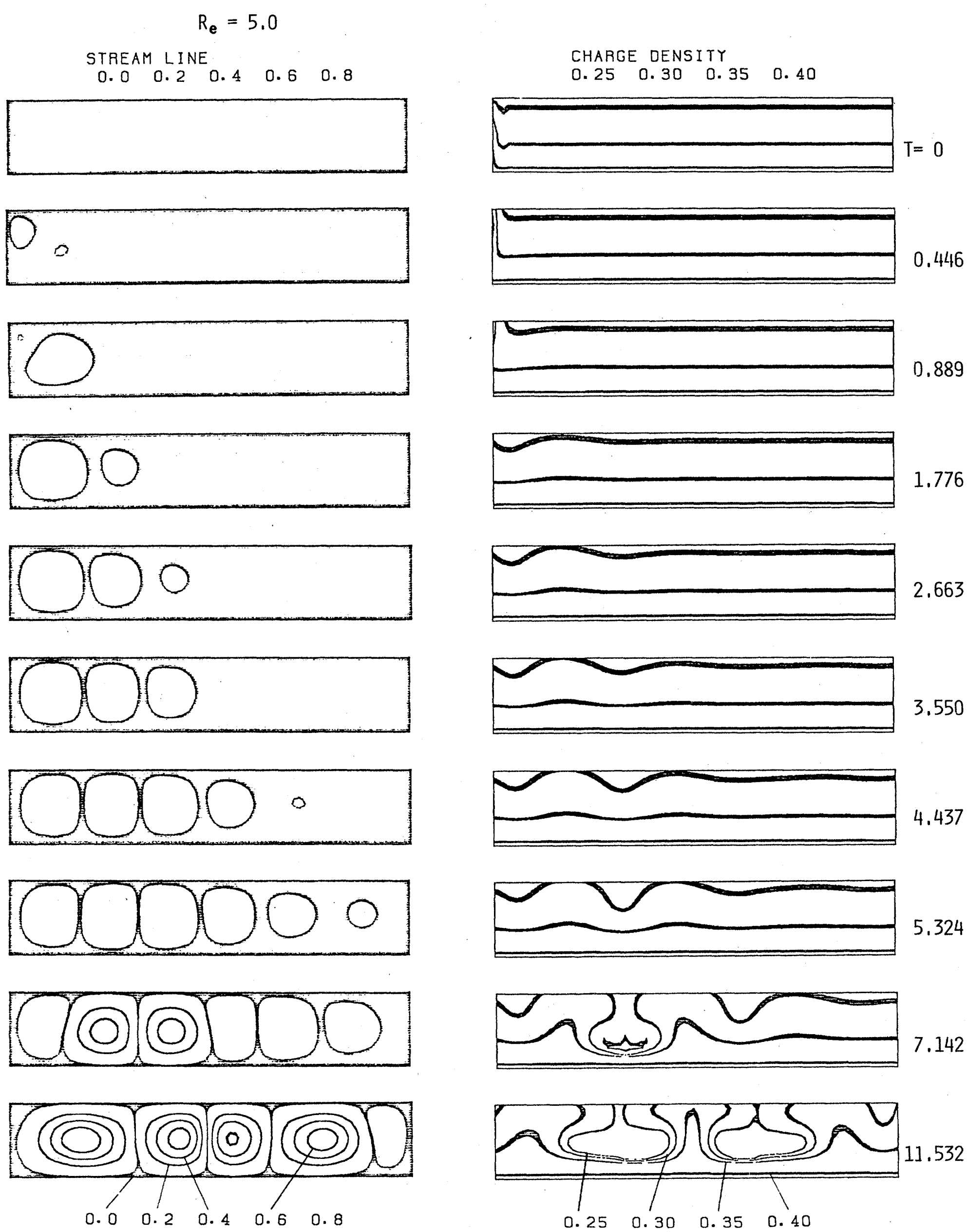

FIG. 3. Propagation of convecting state above the critical point, $R_e=5.0>3.926$.

$$w_0=[W(X,Y,T)e^{i\mathbf{k}\cdot\mathbf{x}}+W^*(X,Y,T)e^{-i\mathbf{k}\cdot\mathbf{x}}]\sin\left[\frac{\pi z}{d}\right],$$

$$q_0=\frac{g_0}{\gamma E_0}[W(X,Y,T)e^{i\mathbf{k}\cdot\mathbf{x}}+W^*(X,Y,T)e^{-i\mathbf{k}\cdot\mathbf{x}}]\sin\left[\frac{\pi z}{d}\right],\quad \mathbf{k}\cdot\mathbf{x}=k_x x+k_y y \tag{2.18}$$

where the amplitude W is a slowly varying function of time and position. The appropriate scaling is

$$X=\epsilon x,\quad Y=\epsilon y,\quad T=\epsilon^2 t\ . \tag{2.19}$$

With this transformation the operators reduce to

$$\frac{\partial}{\partial t}\to\frac{\partial}{\partial t}+\epsilon^2\frac{\partial}{\partial T},$$

$$\nabla_{1\mathbf{x}}\to\nabla_{1\mathbf{x}}+\epsilon\nabla_{1\mathscr{X}},\quad \nabla_{1\mathbf{x}}=\left[\frac{\partial}{\partial x},\frac{\partial}{\partial y}\right],\quad \nabla_{1\mathscr{X}}=\left[\frac{\partial}{\partial X},\frac{\partial}{\partial Y}\right]. \tag{2.20}$$

We expand the dependent variables and the operators as a power series in ϵ,

$$f=\epsilon f_0+\epsilon^2 f_1+\epsilon^3 f_2+\cdots,\quad f=(u,v,w,q,p)\ ,$$

$$\mathscr{L}=\mathscr{L}_0+\epsilon\mathscr{L}_1+\epsilon^2\mathscr{L}_2+\cdots\ . \tag{2.21}$$

Then Eq. (2.17) becomes

$$(\mathscr{L}_0+\epsilon\mathscr{L}_1+\epsilon^2\mathscr{L}_2)(w_0+\epsilon w_1+\epsilon^2 w_2)=-\frac{E_0}{\rho}\epsilon(\nabla_{1\mathbf{x}}^2+2\epsilon\nabla_{1\mathbf{x}}\cdot\nabla_{1\mathscr{X}})[\mathbf{u}_0\cdot\nabla q_0+\epsilon(\mathbf{u}_1\cdot\nabla q_0+\mathbf{u}_0\cdot\nabla q_1)]$$
$$+\epsilon\left[\frac{\partial}{\partial t}+\gamma\right]\{\tilde{\nabla}\times\tilde{\nabla}\times[(\mathbf{\Omega}_0\times\mathbf{u}_0)+\epsilon(\mathbf{\Omega}_1\times\mathbf{u}_0)+\epsilon(\mathbf{\Omega}_0\times\mathbf{u}_1)]\cdot\hat{z}\}\ , \tag{2.22}$$

$$\mathscr{L}_0=\left[\frac{\partial}{\partial t}-\nu\nabla^2\right]\left[\frac{\partial}{\partial t}+\gamma\right]\nabla^2-\frac{g_0}{\rho}\nabla_{1\mathbf{x}}^2\ ,$$

$$\mathscr{L}_1=2\left[\left[\frac{\partial}{\partial t}-\nu\nabla^2\right]\left[\frac{\partial}{\partial t}+\gamma\right]-\nu\left[\frac{\partial}{\partial t}+\gamma\right]\nabla^2-\frac{g_0}{\rho}\right]\nabla_{1\mathbf{x}}\cdot\nabla_{1\mathscr{X}}\ , \tag{2.23}$$

$$\mathscr{L}_2=\left[\left[\frac{\partial}{\partial t}-\nu\nabla^2\right]\left[\frac{\partial}{\partial t}+\gamma\right]-\nu\left[\frac{\partial}{\partial t}+\gamma\right]\nabla^2-\frac{g_0}{\rho}\right]\nabla_{1\mathscr{X}}^2$$
$$+\left[2\frac{\partial}{\partial t}+\gamma-\nu\nabla^2\right]\nabla^2\frac{\partial}{\partial T}-4\nu\left[\frac{\partial}{\partial t}+\gamma\right]\left[\nabla_{1\mathbf{x}}\cdot\nabla_{1\mathscr{X}}\right]^2-\frac{g_2}{\rho}\nabla_{1\mathbf{x}}^2\ ,$$

where $g=g_0+\epsilon^2 g_2$ and $\tilde{\nabla}=\nabla_{1\mathbf{x}}+\epsilon\nabla_{1\mathscr{X}},\partial/\partial z$. The linear balance, $\mathscr{L}_0 W_0=0$, gives the neutral solutions. The neutral condition is that

$$g=\rho\nu\gamma\frac{1}{k^2}\left[k^2+\frac{\pi^2}{d^2}\right]^2. \tag{2.24}$$

At the critical point the wave number is $k_c=\pi/d$ and

$$g_0=4\pi^2\rho\nu\gamma/d^2\ . \tag{2.25}$$

Here we note that our analysis is valid near the critical point; then Eq. (2.25) justifies neglecting the ionic diffusion terms in (2.2) and (2.3).

The first nonlinear response generates second harmonics. However, we can find $\mathscr{L}_1 W_0=0$ at the critical condition. The second harmonic responses denoted by $f_1^{(2)}$ are as follows:

$$W_1^{(2)}=u_1^{(2)}=v_1^{(2)}=0\ ,$$

due to (2.12),

$$q_1^{(2)}=-\frac{2\pi g_0}{\gamma^2 E_0 d}WW^*\sin\left[\frac{2\pi z}{d}\right], \tag{2.26}$$

due to (2.15).

The other modes do not give secular responses in W_2 so that they do not affect the analysis to this stage. The $O(\epsilon^2)$ balance of (2.22) yields

$$\mathscr{L}_0 W_2 = -\mathscr{L}_2 W_0 + \frac{2\pi^2 g_0 k_c^2}{\rho\gamma^2 d^2} W W^* W_0 + \cdots \tag{2.27}$$

where the ellipses represents terms of higher harmonics, with the boundary conditions

$$W_2 = 0,\ \ D^2 W_2 = 0,\ \ D^4 W_2 = 0 \ . \tag{2.28}$$

The second term of the rhs of (2.27) which involves the natural eigenfunction of $\mathscr{L}_0$ should be produced from $\mathscr{L}_2 W_0$ at $\partial/\partial t \to 0$

$$\hat{\mathscr{L}}_2 W = \frac{2\pi^2 g_0 k_c^2}{\rho\gamma^2 d^2} W^2 W^* \ , \tag{2.29}$$

where $\hat{\mathscr{L}}_2$ means $\mathscr{L}_2$ at $\partial/\partial t \to 0$. Finally we obtain

$$\begin{aligned} &\frac{\partial W}{\partial T} - A^2 \frac{\partial^2 W}{\partial X^2} = B^2 (C^2 \chi - W W^*)/W \ , \\ &A^2 = 2\nu\gamma/(\gamma + 2\pi^2 \nu/d^2) \ , \\ &B^2 = \pi^2 g_0/\rho\gamma^2 d^2 (\gamma + 2\pi^2 \nu/d^2) \ , \\ &C^2 = d^2\gamma^2/2\pi^2 \ , \end{aligned} \tag{2.30}$$

where $\chi = g_2/g_0 = (g - g_0)/g_0$. Equation (2.30) can be normalized as

$$\frac{\partial W'}{\partial T'} - \frac{\partial^2 W'}{\partial X'^2} = (1 - W' W'^*) W' \ , \tag{2.31}$$

where $W' = W/c\sqrt{\chi}$, $X' = XBC\sqrt{\chi}/A$, and $T' = TB^2C^2\chi$. Equation (2.31) has the definite propagation velocity of 2.0 which was numerically obtained as in Fig. 1. Thus the propagation velocity v_p for (2.30) is given by $2ABC\sqrt{\chi}$.

C. Example

For a dielectric liquid we choose Pyralene 1500 with the following constants:

$$\begin{aligned} &\rho = 10^3\ \text{kg/m}^3 \ , \\ &\eta = 0.02\ \text{kg/m·s} \ , \\ &\mu = 1.6 \times 10^{-9}\ \text{m}^2/\text{v·s} \ , \\ &d = 0.005\ \text{m} \ , \\ &\epsilon = 5.3 \times 10^{-11}\ \text{F/m} \ . \end{aligned}$$

The parameters satisfying WR and WI conditions are

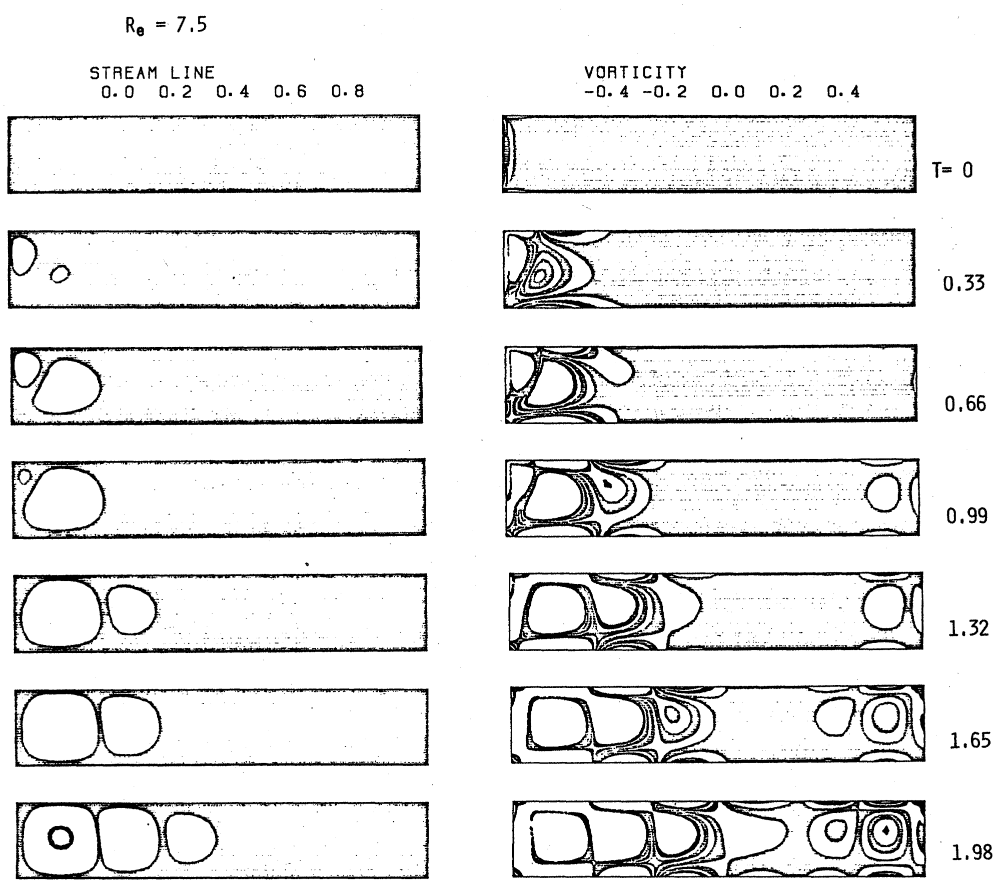

FIG. 4. Propagation of convecting state above the critical point, $R_e = 7.5$.

$E_0 = 4.7\times 10^6$ V/m ,

$n_0 = 3.1\times 10^{17}\ \mathrm{m}^{-3}$,

$\alpha = 2.4\times 10^{-19}\ \mathrm{m}^3/\mathrm{s}$,

$\gamma = 148$ 1/s ,

$g_0 = 4.7\times 10^6\ \mathrm{kg/m^3\,s^2}$.

Then

$$A^2 = 3.6\times 10^{-5},\quad B^2 = 510,\quad C^2 = 2.8\times 10^{-2}$$

so that

$$|W| = 0.167\sqrt{\chi}\ \text{and}\ v_p = 0.045\sqrt{\chi}$$

in m/s.

III. A UNIPOLAR INJECTION TYPE WITH RIGID-RIGID BOUNDARIES

A. Model specifications: An asymmetrical case

Let us consider an incompressible Newtonian dielectric liquid layer held in a two-dimensional container of the aspect ratio 1, the depth, to 5, the width. Unipolar ions are injected to the liquid uniformly from one electrode at $z=0$, and collected by the other electrode at $z=d$, where the electric potential is V_0 at $z=0$, and 0 at $z=d$. The walls are all rigid. At a supercritical condition convection is naturally generated at the side walls because of the inhomogeneity and finally occupies the entire space. The time required for this depends on the magnitude of the inhomogeneity. If a sufficient trigger was given at a side wall we could see the growing process of the convecting state. The processes have numerically been analyzed in the following section.

B. Numerical analysis

The equations of motion for the fluid and the space charge are given with nondimensional variables as follows:

$$x_i' = x_i/d,\quad t' = t\kappa V_0/d^2,\quad \mathbf{E}' = \mathbf{E}d/V_0\ ,$$

$$\Phi' = \Phi/V_0,\quad \epsilon' = \epsilon/\bar{\epsilon},\quad q' = qd^2/\epsilon V_0\ ,$$

$$\mathbf{j}' = \mathbf{j}d^3/\epsilon\kappa V_0^2,\quad p' = pd^2/\rho\kappa^2 V_0^2\ ,$$

$$\mathbf{u}' = \mathbf{u}d/\kappa V_0\ ,$$

$$\frac{\partial\omega}{\partial t} = -\left[\frac{\partial\Psi}{\partial z}\frac{\partial\omega}{\partial x} - \frac{\partial\Psi}{\partial x}\frac{\partial\omega}{\partial z}\right] + \frac{1}{R_e}\Delta\omega + M^2\left[-\frac{\partial q}{\partial z}\frac{\partial\Phi}{\partial x} + \frac{\partial q}{\partial x}\frac{\partial\Phi}{\partial z}\right], \qquad (3.1)$$

where

$$\boldsymbol{\omega} = \nabla\times\mathbf{u},\quad \boldsymbol{\omega} = (0,\omega,0)\ ,$$

$$\mathbf{u} = \left[\frac{\partial\Psi}{\partial z}, 0, \frac{-\partial\Psi}{\partial x}\right],\quad M = (\epsilon/\rho)^{1/2}/\kappa\ ,$$

$$\Delta\Psi = \omega,\quad R_e = \kappa V_0/\nu\ ,$$

$$\frac{\partial q}{\partial t} = -\nabla\cdot[q(\mathbf{E}+\mathbf{u})],\quad T = M^2 R_e\ ,$$

$$\Delta\Phi = -q\ ,$$

with the boundary conditions,

$$\Psi = 0\ \text{for}\ z=0,\ z=1,\ x=0,\ \text{and}\ x=5\ ,$$

$$\omega_w = \frac{3}{h^2}\Psi_{\omega+1} + \tfrac{1}{2}\omega_{w+1} + O(h^2)\ ,$$

$$q = q_0\ \text{at}\ z=0\ ,$$

$$q_w = 4(q_{w\pm1} + q_{w\pm3}) - 6q_{w\pm2} - q_{w\pm4}\quad \text{at}\ x=0,\ x=5,\ \text{and}\ z=1\ , \qquad (3.2)$$

$$\Phi = 1\ \text{at}\ z=0\ ,$$

$$\Phi = 0\ \text{at}\ z=1\ ,$$

and

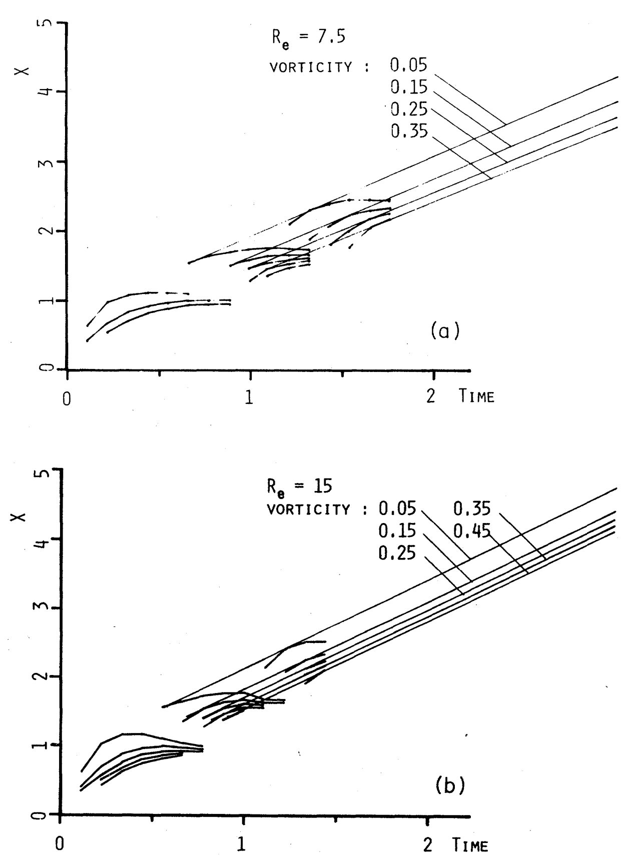

FIG. 5. Motions of contours of vorticity. (a) $R_e = 7.5$, (b) $R_e = 15$.

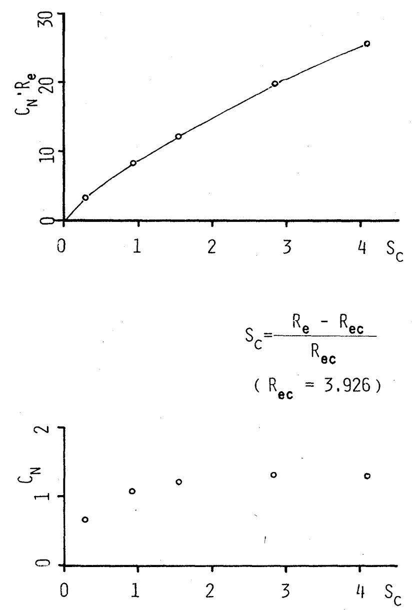

FIG. 6. Propagation velocity of convecting state. C_N is the nondimensional propagation velocity normalized by the ionic drift velocity μE_0. R_e is the electric Reynolds number, where the standard velocity is the ionic drift velocity μE_0, too.

$$\Phi_w = 4(\Phi_{w\pm1} + \Phi_{w\pm3}) - 6\Phi_{w\pm2} - \Phi_{w\pm4} \quad \text{at } x = 0 \text{ and } x = 5 ,$$

where Ψ, w, Φ, and q are the stream function, the vorticity, the electric potential, and the space charge, respectively. ρ, κ, and ν are the liquid density, the ionic mobility, and the kinetic viscosity, respectively. The stationary solution, which is obtained analytically and unstable above the critical point, was chosen as the initial state after adding local space charge near the left wall as the trigger. The above equation set was solved numerically using the Crank-Nicholson method for the vorticity and the donor-cell method for the space charge in the 15×75 mesh scheme. The detailed process can be seen in Ref. 8 by Suzuki and Sawada.

C. Results

The critical condition of our case, which is characterized by the nondimension charge density of 0.410, is known by the linear-stability analysis by Atten and Moreau as $R_e = 3.926$. Below the critical point $R_e = 3.5$ a convection was generated temporarily, but vanished afterward without propagation as in Fig. 2. Above the critical point, propagating transitions from the stationary state to the convecting state have been shown as in Figs. 3 and 4. In order to find the propagation velocity, we plotted the positions of the contours of the vorticity in Fig. 5. Since the tangent lines for contours of the same value are parallel, we can conclude that the convecting state propagates to the outer space with definite velocities. The propagation velocity depends on $(R_e - R_{ec})/R_{ec}$ as in Fig. 6.

IV. CONCLUSION

Here we have used two models as electroconvection systems. One model was chosen as an analytical example and the other as a rather realistic one. The first model was found to have features so close to Rayleigh-Bénard convection that it could be analyzed using the amplitude equation approach. The second model was not only asymmetrical but also subjected to the rigid boundary conditions so that the analysis was thought to be complicated. Then a numerical approach was carried out. In both models propagating transitions with the definite velocities have been found at the supercritical conditions.

ACKNOWLEDGMENTS

The author wishes to thank Professor Y. Sawada, Dr. M. Matsushita, and Dr. Y. Tsutsui for helpful discussions. It is a pleasure to acknowledge the hospitality of the members of Fundamental Department, especially those of the Fluidics Division.

[1]A. C. Newell and J. A. Whitehead, J. Fluid Mech. **38**, 279 (1969).

[2]M. C. Cross, Phys. Rev. A **25**, 1065 (1982).

[3]H. S. Greenside and W. M. Coughran, Phys. Rev. A **30**, 398 (1984).

[4]G. Ahlers and D. S. Cannell, Phys. Rev. Lett. **50**, 1583 (1983).

[5]P. Atten and R. Moreau, J. Mec. **11**, 471 (1972).

[6]J. C. Lacroix, P. Atten, and E. J. Hopfinger, J. Fluid Mech. **69**, 539 (1975).

[7]N. Felici and J. C. Lacroix, J. Electrostat. **5**, 135 (1978).

[8]M. Suzuki and Y. Sawada, Phys. Rev. A **27**, 478 (1983).